Thermopower across the insulator-metal divide in $NiCr_{2-x}V_xS_4$ ($0 \leqslant x \leqslant 2$)

Anthony V. Powell,[1,*] Paz Vaqueiro,[1] and Tsukio Ohtani[2]
[1]*Department of Chemistry, Heriot-Watt University, Edinburgh EH14 4AS, United Kingdom*
[2]*Laboratory for Solid-State Chemistry, Okayama University of Science, 1-1Ridai-cho, Okayama 700-005, Japan*
(Received 27 September 2004; published 22 March 2005)

Measurements of the Seebeck coefficient of phases in the series $NiCr_{2-x}V_xS_4$ have been carried out over the temperature range $90 \leqslant T/K \leqslant 700$. The data demonstrate that with increasing levels of vanadium incorporation, there is a change from semiconducting to metallic behavior at a critical composition $0.4 \leqslant x_c \leqslant 0.5$. This change in the nature of the electronic states is coincident with a structural distortion, previously identified by powder neutron diffraction, involving the formation of zigzag cation chains within a dichalcogenide slab. Analysis of the temperature dependence of the thermopower in the semiconducting and metallic regions suggests that the transport properties are strongly affected by electron-phonon coupling, which for $x \leqslant 0.2$ leads to a small-polaron hopping conduction mechanism. Analysis of the conductivity data yields activation energies of 28.1(1) and 60.3(3) meV for $x=0.0$ and 0.2, respectively.

DOI: 10.1103/PhysRevB.71.125120 PACS number(s): 71.30.+h, 72.80.Ga, 71.38.−k

INTRODUCTION

The insulator to metal (ITM) transition is of fundamental importance in condensed-matter science[1] and encompasses phenomena as diverse as metallization processes in stars and size-induced transitions in microscopic metal particles. From a chemical perspective, materials which lie close to the MI divide are of immense interest owing to the unique properties which they frequently exhibit and the opportunities afforded to tailor such properties using chemical control. For example, it has been suggested that the remarkable superconducting properties of the cuprates result from them being on the borderline of electron localization.[2] In addition, the exceptional magnetotransport properties exhibited by mixed manganese perovskites are most marked at temperatures close to that of a MI transition.[3]

Our recent investigations have been directed towards mixed-metal sulphides which lie in this important region of the electronic phase diagram.[4–6] Much of our work has involved an examination of the effects of chemical substitution in materials which adopt the monoclinic Cr_3S_4 structure.[7–10] This is one of a range of ordered defect structures that may be derived from that of nickel arsenide by removal in an ordered manner of a fraction of the cations between alternate pairs of anion layers.[11] The Cr_3S_4 structure[12] corresponds to a cation deficiency of 25%. Vacancies are confined to layers of octahedral sites between alternate pairs of anion layers, with the result that the structure may be seen to consist of dichalcogenide (MS_2) units of edge-linked MS_6 octahedra, separated by cation-deficient layers (Fig. 1). Ordering of the vacancies in these defective layers produces a two-dimensional superstructure with dimensions related to those of the primitive hexagonal unit cell (a_p) by $\sqrt{3}a_p \times a_p$. There are two crystallographically distinct cation sites, as indicated by the formulation $(M)[M_2]S_4$, where (M) and $[M]$ denote sites in the vacancy and fully occupied layers, respectively. For ternary phases AM_2S_4, two extreme cation distributions are possible, corresponding to the normal, $(A)[M_2]S_4$, and inverse $(M)[AM]S_4$ structure types.

We have recently demonstrated[13–15] through a series of x-ray and neutron diffraction studies that cation partitioning is seldom complete and, in ternary phases containing first-row transition metals, the cation distribution is dependent on the electronic properties of the constituent cations. In particular, cations drawn from the early part of the transition series show a greater preference for sites in the fully occupied layer. This may be related to the ability of such cations to delocalize electron density by direct t_{2g}-t_{2g} interactions. Recognizing this correlation has enabled us to design series of materials in which substitution may be effected selectively

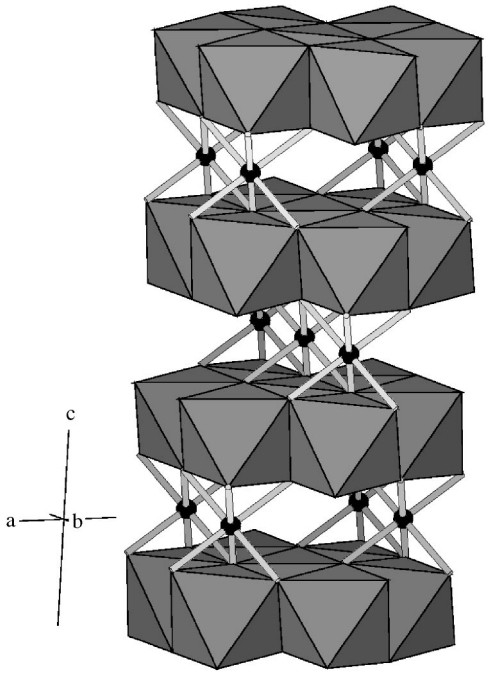

FIG. 1. The ordered-defect Cr_3S_4 structure adopted by materials of stoichiometry AB_2S_4. Cations in the fully occupied layer lie at the center of shaded MS_6 octahedra, which form a layer of stoichiometry MS_2. Cations in the defect layer are represented by solid circles.

 ©2005 The American Physical Society

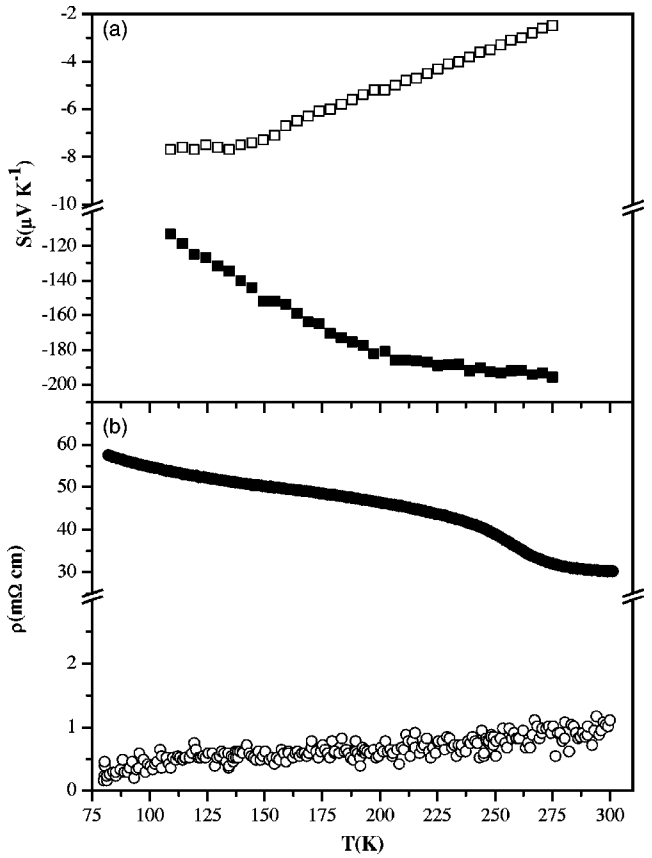

FIG. 2. Contrasting transport properties of the end-member phases $NiCr_2S_4$ (solid points) and NiV_2S_4 (open points): (a) Seebeck coefficient and (b) resistivity.

at one site. In the series $NiCr_{2-x}V_xS_4$, this allowed us to study[8] the change in electron transport properties of semiconducting $NiCr_2S_4$, as chromium in the dichalcogenide layer is progressively replaced with vanadium to give, ultimately, metallic NiV_2S_4.

The results reveal that the onset of metallic behavior in $NiCr_{2-x}V_xS_4$ ($0 \leqslant x \leqslant 2$) is associated with a structural distortion involving the formation of zigzag chains of cations within the dichalcogenide unit. However, as indicated in our previous study,[8] while the temperature dependence of the resistivity clearly shows that the metallic behavior of NiV_2S_4 persists to $x=0.8$ and that all phases with $x \leqslant 0.5$ are semiconducting, there is a region of ambiguity that extends over $0.5 < x < 0.8$. In this region $d\rho/dT$ is small and positive down to ca. 40 K, which is consistent with metallic behavior, but on further cooling the resistivity shows a slight increase. We attributed this effect to the dominance at low temperatures of extrinsic contributions to the bulk resistance: in particular grain boundary effects arising from the polycrystalline nature of the materials. However, given that the onset of the structural distortion occurs precisely in the region where the transport behavior is not well defined, it is desirable to find an alternative probe of the nature of the electronic states. The Seebeck coefficient (S) has been shown to be less sensitive than resistance measurements to grain boundary effects in polycrystalline materials, because the temperature drop between grains is less significant than the voltage drop. Therefore, in an effort to elucidate the nature of the electronic properties in the vicinity of the structural distortion, the Seebeck coefficient has been determined as a function of temperature for a range of compositions in the series $NiCr_{2-x}V_xS_4$ ($0 \leqslant x \leqslant 2$). The results demonstrate that the structural distortion is coincident with the insulator-metal transition but also reveal that the $S(T)$ dependence is not that of a conventional metal or broadband semiconductor.

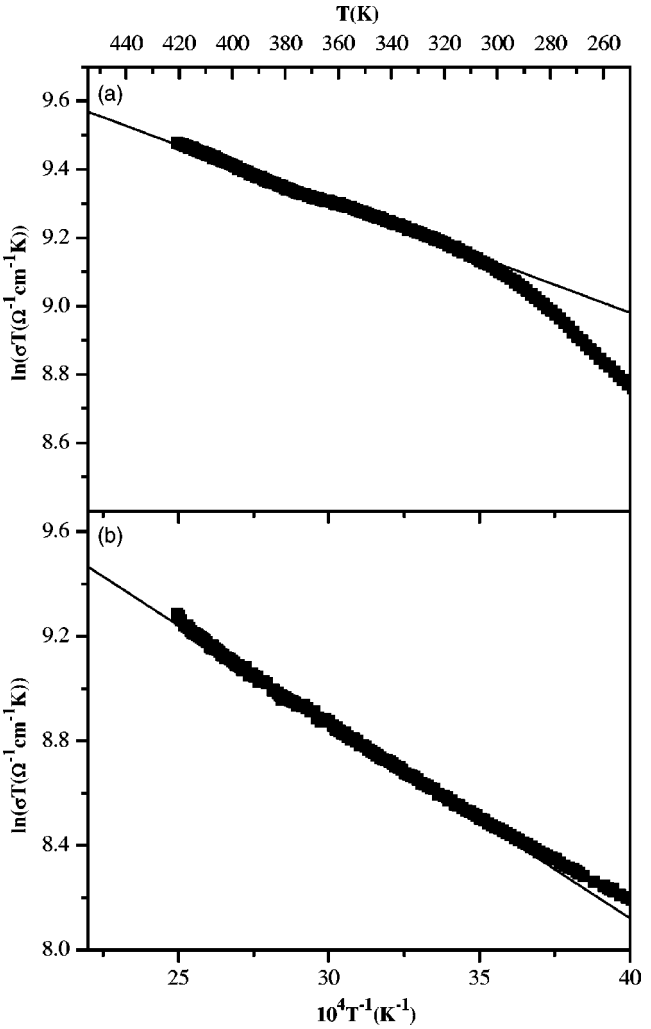

FIG. 3. Conductivity data plotted in the form σT against $1/T$ for (a) $NiCr_2S_4$ and (b) $NiCr_{1.8}V_{0.2}S_4$. The solid line represents the linear fit obtained for a polaronic hopping model, using Eq. (3).

EXPERIMENT

All samples were prepared by high-temperature reaction at 800 °C of appropriate mixtures of the powdered elements in evacuated, sealed silica ampoules. A combination of powder x-ray diffraction, thermogravimetry, and energy-dispersive x-ray microanalysis confirmed all materials to be single phases, with unit-cell parameters consistent with the adoption of a Cr_3S_4-type structure and compositions in good agreement with nominal stoichiometries. Powder neutron diffraction provided detailed structural information and dem-

onstrated that substitution takes place exclusively in the dichalcogenide slab. Full details of the preparation and characterization of these samples have been presented elsewhere.[8]

Measurement of the Seebeck coefficient of $NiCr_{2-x}V_xS_4$ was carried out for several compositions in the range $0 \leqslant x \leqslant 2$, with particular emphasis being given to the region $0.5 < x < 0.8$. Data were collected both on heating and cooling over the temperature range $90 \leqslant T/K \leqslant 270$ using apparatus constructed in-house. However, there was little evidence of hysteresis in the data, and therefore only data from the heating runs are presented here. Copper wires were connected to each end of a sintered ingot (>90% of theoretical density) using gold paste. The sample assembly was enclosed in a glass sheath filled with He exchange gas and the whole immersed in liquid nitrogen. The Seebeck voltage, corrected for the Cu wires, was determined with a temperature differential between the ends of the sample of ca. 4 K using an Okura Electric model AM-1001 microvoltmeter. Additional data were collected at temperatures to 700 K, on both heating and cooling, using a pyrophyllite sample mounting, in which a sintered ingot is sandwiched between two baked pyrophillite plates, contained in a furnace. A temperature gradient of ca. 6 K was measured with a differential *K*-type thermocouple and the Seebeck voltage was measured using gold wires. The gold wires and thermocouples were kept in contact with the sample by the pyrophillite plates. Details of the experimental arrangement have been presented elsewhere.[16]

RESULTS AND DISCUSSION

Stoichiometric $NiCr_2S_4$ is an intrinsic semiconductor in which electron transport requires promotion of electrons from t_{2g}-derived levels of Cr(III) to a conduction band comprised of cation and anion e_g states. While two contributions to the Seebeck voltage, of opposite sign arising from electrons and holes, might be expected, the markedly higher mobility of the electrons in the e_g-derived band causes the conductivity-weighted sum[17] of the two contributions to be dominated by the negative contribution of the electrons. Furthermore, the ca. 2% sulphur deficiency that is necessary for the formation of single-phase material introduces donor levels [formally Cr(II)] below the conduction band, with the result that electrons are the dominant charge carriers. This is reflected in the Seebeck coefficient of $-200\ \mu V\ K^{-1}$ determined at 270 K. This value is in excellent agreement with the value of $-219\ \mu V\ K^{-1}$ at 300 K reported by Albers *et al.*,[18] although it is somewhat larger in magnitude than that reported by Holt *et al.*.[19] This discrepancy may reflect differences in sample preparation, as we have recently shown[20] that disordering of cations in $NiCr_2S_4$ occurs at the high temperatures used in synthesis, leading to differences in physical properties for materials prepared under different rates of cooling. $NiCr_2S_4$ exhibits thermally activated conduction of the Arrhenius type.[21] For a conventional broadband *n*-type semiconductor, the thermopower *S* is given by[22]

$$S = -\frac{k}{e}\left(\frac{E_C - E_F}{k_B T} + A\right), \tag{1}$$

where E_C is the conduction band energy, E_F is the Fermi energy, and *A* is a constant that depends on the nature of the electron scattering process. However, contrary to the temperature dependence expected from Eq. (1), the absolute value of the Seebeck coefficient of $NiCr_2S_4$ increases on warming from 100 to 275 K (Fig. 2). The thermopower shows a linear temperature dependence on warming to 200 K, after which a second linear region, with reduced gradient, is observed. The change in slope at 200 K appears to be related to the onset of long-range magnetic order at T_N, determined as 180(5) K,[21] which has been shown to be accompanied by a decrease in the activation energy for electron transport, indicative of an appreciable contribution to the electrical resistance of spin-disorder scattering of the charge carriers.[21]

The increase in $|S|$ with increasing temperature is the behavior expected for a metal. This indicates that the Fermi level is located within a band of allowed electron states with transport occurring in the vicinity of E_F.[22] The metal-like behavior of *S* suggests that the carrier concentration is constant within the temperature range studied. This is consistent with the majority charge carriers being electrons, promoted from donor levels located at energies below the conduction band which are small compared to *kT*. A constant carrier concentration together with an activated resistivity indicates that it is the mobility that is thermally activated. Activated mobility arises from carrier localization, either due to disorder or electron-phonon coupling (polarons). Charge transport then occurs by hopping between localized states in the vicinity of the Fermi level. Mott and co-workers[23,24] have derived the following expression for the thermopower of such systems:

$$S = -\left(\frac{\pi^2 k_B}{3e}\right)\left(kT\frac{d\ln(\mu_0 N)}{dE} - \frac{dW}{dE}\right). \tag{2}$$

This expression is of the same functional form $(A+BT)$ as that obtained empirically by Wood and Emin[25] for hopping of small polaron holes between inequivalent sites in boron carbides, where $B = kzJ^2/2qW_p^3$ (q is the electronic charge, z the number of nearest neighbors, J the intersite transfer energy, and W_p the small-polaron binding energy). The gradient of $S(T)$ decreases from $-0.79(2)\ \mu V\ K^{-2}$ at $T < 181$ K to $-0.16(1)\ \mu V\ K^{-2}$ above this temperature. We have previously shown that the conductivity of $NiCr_2S_4$ may be described in terms of a simple activated conduction mechanism, with a change in activation energy at the magnetic ordering temperature. From the gradient of the $S(T)$ plot, the quantity J^2/W_p^3 is estimated as $2.7 \times 10^{13}\ erg^{-1}$ above T_N and $1.3 \times 10^{14}\ erg^{-1}$ below it. These values are similar to those obtained for small-polaron conduction in oxides.[26] The small-polaron hopping conduction mechanism implied by the Seebeck data presented here would lead to a slightly different (from Arrhenius behavior) temperature dependence of the conductivity of the form

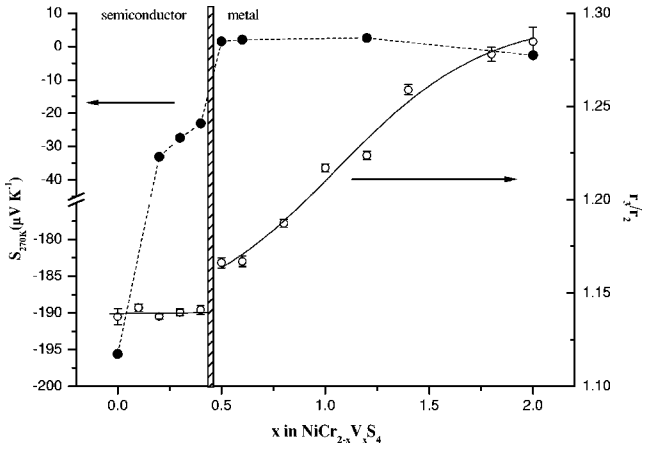

FIG. 4. Comparison of the variation with composition of the Seebeck coefficient at 270 K (solid points) with the structural distortion corresponding to the formation of zigzag chains of cations, indicated by the increase in the ratio r_3/r_2 (open points).

$$\sigma T \propto \sigma_0 \exp(-W_H/kT). \tag{3}$$

The plot of σT vs $1/T$ is linear in the high-temperature region $290 \leqslant T/K \leqslant 400$ (Fig. 3), yielding a hopping energy of 28.1(1) meV. As this is related to the polaron binding energy W_p by $W_p = 2W_H$,[23] an estimate of 87 meV is obtained for the intersite transfer energy J at high temperatures.

By contrast, at 270 K, the other end-member phase NiV_2S_4 exhibits (Fig. 2) a small negative thermopower ($|S| = 2.5\ \mu V\ K^{-1}$), similar to that reported by Bouchard and Wold,[27] which has a less marked temperature dependence to that of $NiCr_2S_4$. Although the resistivity data clearly indicate metallic behavior for NiV_2S_4, $|S|$ does not increase with increasing temperature, as expected for conventional metallic diffusion thermopower,[28] but exhibits an almost linear decrease as the temperature is raised. This behavior has been observed in a number of metallic alloys in which phonon drag is suppressed[29] and, in a more pronounced form, in the cuprate high-temperature superconductors.[30] It has been shown[31] that this anomalous behavior arises from electron-phonon interactions. Strong electron-phonon coupling for some of the carriers enhances the thermopower, introducing into the expression for metallic diffusion thermopower additional terms whose relative weighting varies with temperature. Therefore, we conclude that while NiV_2S_4 may be described as an *n*-type metallic material, it is an unconventional metal in which electron-phonon interactions play an important role. Structural investigations[15] reveal a vanadium-vanadium separation of ca. 2.9 Å within the dichalcogenide unit of NiV_2S_4. This is below the critical distance, R_c, for direct t_{2g}-t_{2g} orbital overlap.[32] The metallic behavior is therefore consistent with the broadening of vanadium t_{2g} levels into a narrow one-dimensional band, which for the stoichiometric material is 2/3 filled.

Between the extremes of the two ternary end-member phases, the compositional variation of the Seebeck coefficient at 270 K is nonlinear (Fig. 4). On doping the metallic phase NiV_2S_4 with chromium, $S_{270\ K}$ initially remains within a few $\mu V\ K^{-1}$ of zero, although the small positive value

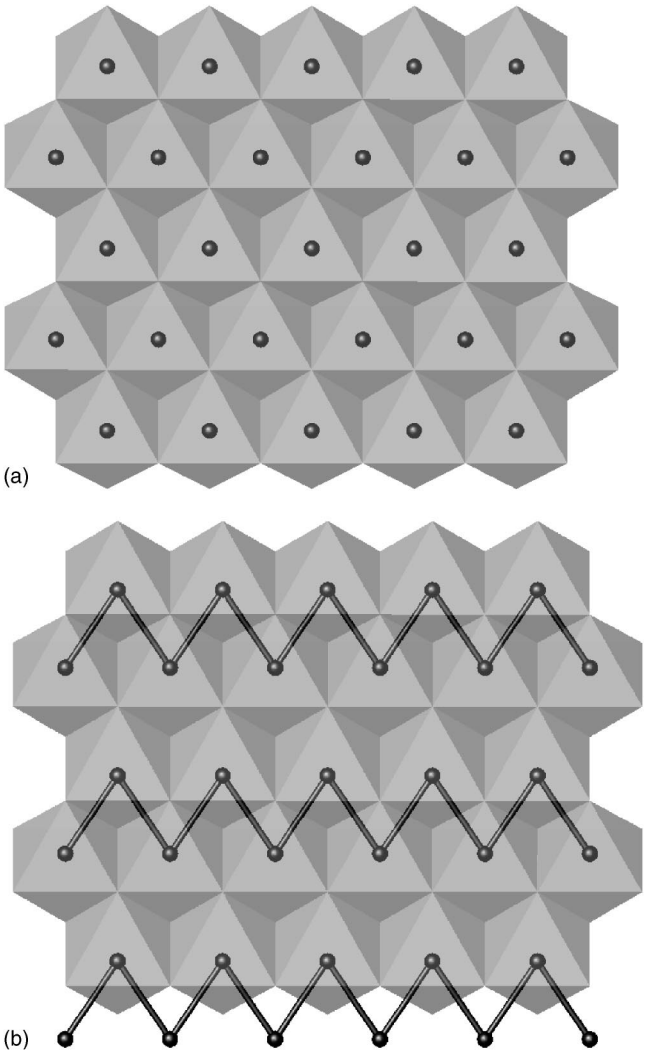

FIG. 5. The structural distortion within the dichalcogenide layer of $NiCr_{2-x}V_xS_4$ ($0 \leqslant x \leqslant 2$): (a) the pseudohexagonal arrangement of cations in the dichalcogenide layer of the undistorted Cr_3S_4 structure and (b) zigzag chains of cations directed along [010]. Solid lines in (b) denote cation-cation distances $\leqslant R_c$.

which it assumes in the doped phases may indicate that hole-type conduction within the narrow t_{2g}-derived band becomes dominant. This behavior persists to $x = 0.5$, but increasing the chromium content further produces a marked increase in $|S|$, the thermopower rapidly becoming more negative. The compositional variation of $S_{270\ K}$ clearly demonstrates that there is a significant change in the electronic states of $NiCr_{2-x}V_xS_4$ between $x = 0.4$ and $x = 0.5$ and suggests that the boundary between localized and itinerant electron states is in the region $0.4 < x < 0.5$. When the compositional dependence of $S_{270\ K}$ is compared with the structural evolution (Fig. 4), it is evident that the change in the nature of the electronic states coincides with the onset of the structural distortion involving formation of zigzag cation chains (Fig. 5), as measured by the ratio r_1/r_3. The intrachain cation-cation separation is below R_c, suggesting that the distortion leads to broadening of vanadium t_{2g} levels into a narrow band, resulting in the transition from semiconducting to metallic behavior.

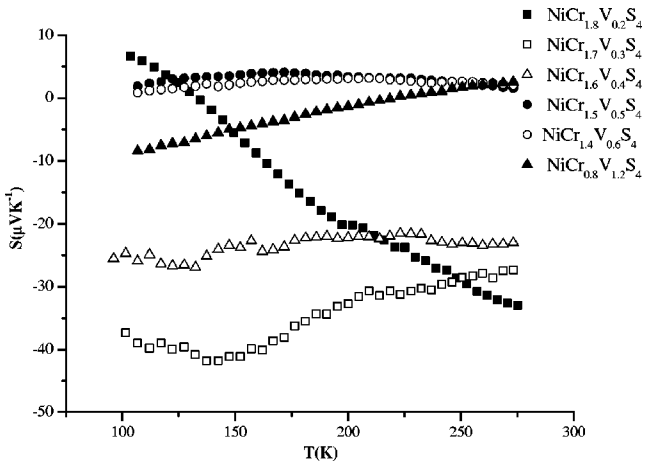

FIG. 6. Seebeck coefficient data for nonstoichiometric materials $NiCr_{2-x}V_xS_4$ $(0.2 \leqslant x \leqslant 1.2)$ collected over the temperature range $90 \leqslant T/K \leqslant 270$.

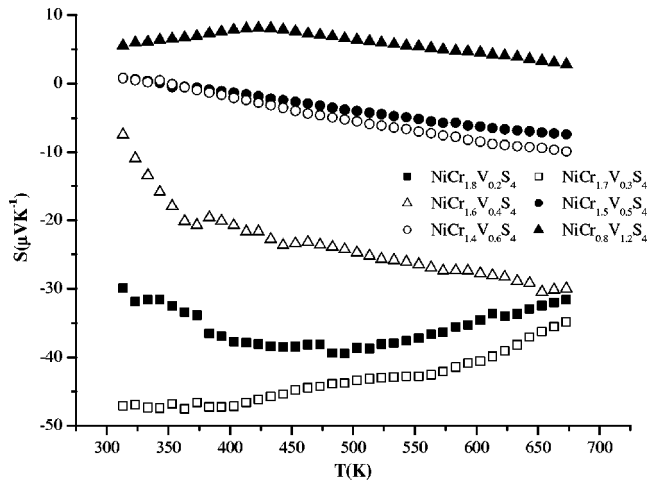

FIG. 7. Seebeck coefficient data for nonstoichiometric materials $NiCr_{2-x}V_xS_4$ $(0.2 \leqslant x \leqslant 1.2)$ collected over the temperature range $310 \leqslant T/K \leqslant 700$.

Interpretation of the temperature dependence of the Seebeck coefficient of the nonstoichiometric phases (Fig. 6) is complicated by the presence of multiple charge-carrier scattering mechanisms. In the present case, three broad categories of behavior may be identified on cooling below room temperature. The thermopower of semiconducting $NiCr_{1.8}V_{0.2}S_4$ in the temperature range $100 \leqslant T/K \leqslant 300$ shows an increase in $|S|$ with increasing temperature similar to that observed for $NiCr_2S_4$. However, the magnitude of S is markedly reduced from that of the end-member phase. As doping involves the substitution of $Cr(III):d^3$ with $V(III):d^2$, it corresponds to the creation of electron-hole pairs in the t_{2g}-derived conduction band. Therefore doping involves an increase in the charge carrier density, which lowers the electrical resistance and, as is observed here, results in a reduction in the Seebeck coefficient. The resistivity data for $NiCr_{1.8}V_{0.2}$ are reasonably well described by a variable-range hopping model,[8] which would lead to a $T^{1/2}$ dependence to the thermopower. However, the behavior of $S(T)$ is similar to that of $NiCr_2S_4$, including a decrease in gradient from $-0.305(5)$ to $-0.186(3)$ $\mu V\,K^{-2}$ in the region of the magnetic ordering temperature at $T_N \approx 190$ K. This suggests that conduction in $NiCr_{1.8}V_{0.2}S_4$ is perhaps also better described as being due to small-polaron hopping, and values of 3.1×10^{13} and 5.1×10^{13} erg^{-1} for J^2/W_p^3 are obtained above and below T_N, respectively. Further evidence for this mechanism is provided by the linearity of the plot of σT vs $1/T$ over a similar range of temperature to that observed for $NiCr_2S_4$ [Fig. 3(b)], yielding an activation energy W_H of 60.3(3) meV.

The thermopower at higher levels of doping $(x=0.3,0.4)$ shows a similar reduction relative to $NiCr_2S_4$ as that observed in $NiCr_{1.8}V_{0.2}S_4$. However, while the magnitude of S remains consistent with the observed semiconducting behavior, the $S(T)$ dependence for these materials is much weaker than for $NiCr_{1.8}V_{0.2}S_4$, $|S|$ varying by less than ± 4 $\mu V\,K^{-1}$ over the entire range of temperature studied. The absolute value of the Seebeck coefficient for materials with $x > 0.5$ is much reduced $(|S| < 10\ \mu V\,K^{-1})$ to values consistent with the description of these materials as poor metals. The temperature dependence of the Seebeck coefficient also shows evidence of significant electron-phonon coupling similar to that of the end-member phase NiV_2S_4, resulting in a change in sign of dS/dT at ca. 200 K for materials with $x=0.5,0.6$.

Seebeck data collected for nonstoichiometric materials at temperatures above ambient (Fig. 7) reveal that at levels of vanadium incorporation, $x \geqslant 0.5$, the materials behave as conventional metals at higher temperatures. Materials with vanadium contents of $x=0.5,0.6$, for which dS/dT changes sign at ca. 200 K, exhibit thermopowers that increase linearly with temperature above ca. 375 K. By contrast, $S(T)$ for $NiCr_{0.8}V_{1.2}S_4$ initially continues the trend established below ambient temperature, the Seebeck coefficient becoming positive above 220 K, until a local maximum is reached at 423 K, above which temperature it shows a linear decrease with increasing temperature.

In conclusion, by using a technique that is less susceptible to intergranular effects than are conductivity measurements on polycrystalline pellets, we have demonstrated that the structural distortion which occurs in $NiCr_{2-x}V_xS_4$ at $0.5 < x_c < 0.6$ is coincident with a marked change in electronic states. However, both semiconducting and metallic materials exhibit unconventional behavior due to the effects of electron-phonon coupling. We are currently using chemical substitution to tune the structure of the dichalcogenide block in ordered-defect sulphides and have recently demonstrated[33] that a change from triangular clustering to zigzag chains, with an accompanying change in transport properties, may be induced by progressive substitution of molybdenum in VMo_2S_4 by vanadium, indicating that the formation of such chains is intimately linked to metallization.

ACKNOWLEDGMENT

We thank The Royal Society for supporting this work through the award of a Joint Project Grant.

*Corresponding author. FAX: +44 (0)131 451 3180. Electronic address: a.v.powell@hw.ac.uk

[1] P. P. Edwards, R. L. Johnston, F. Hensel, C. N. R. Rao, and D. P. Tunstall, Solid State Phys. **52**, 229 (1999).
[2] P. P. Edwards, T. V. Ramakrishnan, and C. N. R. Rao, J. Phys. Chem. **99**, 5228 (1995).
[3] M. B. Salamon and M. Jaime, Rev. Mod. Phys. **73**, 583 (2001).
[4] P. Vaqueiro, M. L. Kosidowski, and A. V. Powell, Chem. Mater. **14**, 1201 (2002).
[5] P. Vaqueiro, A. V. Powell, A. I. Coldea, C. Steer, I. M. Marshall, S. J. Blundell, J. Singleton, and T. Ohtani, Phys. Rev. B **64**, 132402 (2001).
[6] P. Vaqueiro, A. V. Powell, S. Hull, and D. A. Keen, Phys. Rev. B **63**, 064106 (2001).
[7] P. Vaqueiro and A. V. Powell, Chem. Mater. **12**, 2705 (2000).
[8] P. Vaqueiro, M. Bold, A. V. Powell, and C. Ritter, Chem. Mater. **12**, 1034 (2000).
[9] A. V. Powell, D. C. Colgan, and C. Ritter, J. Solid State Chem. **143**, 163 (1999).
[10] A. V. Powell and S. Oestreich, J. Mater. Chem. **6**, 807 (1996).
[11] A. Kjeshus and W. B. Pearson, Prog. Solid State Chem. **1**, 83 (1964).
[12] F. Jellinek, Acta Crystallogr. **10**, 620 (1957).
[13] D. C. Colgan and A. V. Powell, J. Mater. Chem. **6**, 1579 (1996).
[14] D. C. Colgan and A. V. Powell, J. Mater. Chem. **7**, 2433 (1997).
[15] A. V. Powell, D. C. Colgan, and P. Vaqueiro, J. Mater. Chem. **9**, 485 (1999).
[16] T. Ohtani, K. Kuroda, K. Matsugami, and D. Katoh, J. Eur. Ceram. Soc. **20**, 2721 (2000).
[17] G. S. Nolas, J. Sharp, and H. J. Goldsmid, in *Thermoelectrics: Basic Principles and New Materials Developments* (Springer-Verlag, Berlin, 2001), Chap. 2.
[18] W. Albers, G. van Aller, and C. Haas, Propriétes Thermodynamiques, Physiques et Structurales des Dérivés Semi-Métalliques, CNRS, (1967), p. 19.
[19] S. L. Holt, R. J. Bouchard, and A. Wold, J. Phys. Chem. Solids **27**, 755 (1966).
[20] P. Vaqueiro, S. Hull, B. Lebech, and A. V. Powell, J. Mater. Chem. **9**, 2859 (1999).
[21] A. V. Powell, D. C. Colgan, and C. Ritter, J. Solid State Chem. **134**, 110 (1997).
[22] N. F. Mott and E. A. Davis, *Electronic Processes in Non-Crystalline Materials*, 2nd ed. (Clarendon Press, Oxford, 1979).
[23] L. G. Austin and N. F. Mott, Adv. Phys. **18**, 41 (1969).
[24] M. Cutler and N. F. Mott, Phys. Rev. **181**, 1336 (1969).
[25] C. Wood and E. Emin, Phys. Rev. B **29**, 4582 (1984).
[26] W. H. Jung, H. Wakai, H. Nakatsugawa, and E. Iguchi, J. Appl. Phys. **88**, 2560 (2000).
[27] R. J. Bouchard and A. Wold, J. Phys. Chem. Solids **27**, 591 (1966).
[28] A. T. Burkov and M. V. Vedernikov, in *CRC Handbook of Thermoelectrics*, edited by D. M. Rowe (CRC Press, Boca Raton, 1995), Chap. 32.
[29] M. A. Howson and B. L. Gallagher, Phys. Rep. **170**, 265 (1988).
[30] A. B. Kaiser and C. Uher, in *Studies of High Temperature Superconductors*, edited by A. V. Narlikar (Nova, Commack, NY, 1990).
[31] A. B. Kaiser and G. Mountjoy, Phys. Rev. B **43**, 6266 (1991).
[32] J. B. Goodenough, *Magnetism and the Chemical Bond* (Wiley, New York, 1963).
[33] A. V. Powell, A. McDowall, P. Vaqueiro, R. I. Smith, T. Ohtani, and Y. Okuya, J. Mater. Chem. **14**, 3051 (2004).